View metadata, citation and similar papers at core.ac.uk
brought to you by CORE
provided by Ministry of Earth Sciences, Government of India

Author version: *Int. J. Remote Sens., vol.33 (7); 2011; 1991-2002*

Does sea level pressure modulate the dynamic and thermo-dynamic forcing in the tropical Indian Ocean?

P.G. NISHA†, P.M. MURALEEDHARAN*†, M.G. KEERTHI†, P.V. SATHE†, M.RAVICHANDRAN‡

† National Institute of Oceanography, Dona Paula, Goa 403 004, India

‡ Indian National Centre for Ocean Information Services (INCOIS), India

*Corresponding author. Email address: murali@nio.org

Abstract

Daily fields of sea surface temperature (SST), wind speed (WS) and rainfall are downloaded from the TMI site. Humidity fields are retrieved from SSMI brightness temperature data.. Other variables like solar radiation, back radiation, air temperatures, sea level pressure (SLP) etc required for the computation of latent heat flux (LHF) were taken from ECMWF daily reanalysis fields. All data were transformed into one degree gridded ensembles to generate pentads to compute LHF. Three areas viz; North Indian Ocean (NIO), Equatorial Indian Ocean (EIO), South Indian Ocean (SIO) was chosen over the tropical Indian Ocean to investigate the dependency of SST, WS and SLP on LHF. The dynamic and thermo dynamic behavior of the tropical Indian Ocean was studied from the trends of the scatter represented by the mean and standard deviation of LHF, WS and Dq binned in 1 C SST interval plotted against SST. The direct linear relationship of LHF with SST reverses at some point to display an inverse relationship when the atmosphere is coupled with the ocean. The point at which the reversal takes place marks the threshold SST which appears to have an inherent relationship with the SLP especially when the ocean-atmosphere system is coupled. North of 5 S, the LHF peaks at the threshold SST of 27.5 C and decreases gradually on either side. The resemblance of SST-LHF curve of SIO & EIO with that of the equatorial Pacific can be attributed to the fact that both regime fell under the same pressure band that covers the equatorial Pacific. Shifting of LHF maxima to lower SST regime as SLP increases is noticed at southern and northern latitudes while such regime shift is not noticed at the equator. This phenomenon can be attributed to relatively weaker air sea coupling and subsequent lower LHF production at the equatorial India Ocean.

1. Introduction

Dynamical and thermo dynamical behavior of the tropical Indian Ocean is significantly different from other major oceans as it experiences periodical reversal of winds associated with the meridional oscillation of Inter Tropical Convergence Zone (ITCZ). The periodic meridional shifting of pressure bands in association with the thermal forcing (ITCZ) appears to have impact on the ocean-atmosphere coupling process. The ocean atmosphere coupling reaches at its peak when the LHF is maximum. The relationship between SST and the Latent Heat Flux (LHF) was thought to be straightforward as SST increases, the saturation water vapor mixing ratio increases exponentially. Therefore it is relatively easy to understand the role of thermodynamics in the formation of LHF. The role of atmospheric dynamics coupled with SST to regulate LHF is relatively complicated. From simple analysis of moist static energy of the surface air, Ramnathan and Collins 1992 had shown that at high SST (> 300 K) the surface air is convectively unstable. Areas that are convectively unstable are subject to low level convergence and at the center of convergence the wind speed is low thereby limiting LHF (Neelin and Held 1987; Liu 1988). Therefore at high SSTs the LHF is primarily determined by dynamics. Using a coupled atmosphere-ocean boundary layer model, Sui et al., 1991 demonstrated that the characteristics of the LHF can change significantly with or without the coupling between atmospheric and oceanic boundary layer. In their experiments, when both the SST and the surface wind are prescribed (i.e., no interaction between the SST and the surface wind is allowed) the LHF is found to increase with SST due to the increase of humidity difference. Observations of Zang and Mc Phaden 1995 at the equatorial Pacific indicate similar trends in the low SST regime (< 300 K) which is consistent with the thermodynamic consideration. However at SSTs above 300 K, LHF decreases with increasing SST as a result of dynamic interaction between the large scale circulation and SST. Nevertheless the authors caution that convection is not always responsible directly for the small LHF. Instead, for short period of time in convective regions, surface sensible and latent heat flux may be significantly enhanced due to high wind speeds at gust fronts and high humidity difference as a result of dry and cold convective-scale downdrafts. Laird and Kristovich 2002 has examined one of such short term seasonal fluctuations of surface heat fluxes measured by a moored buoy over the Great Lakes and their relation to synoptic weather events (sea level pressure). The magnitude of surface sensible and latent heat fluxes remained coupled to transient synoptic-scale weather events with maximum (minimum) surface heat fluxes followed the passage of low (high) pressure. The linkage between the surface processes and the synoptic weather pattern is not well understood over Oceans and any attempt in this line would be useful for both weather forecasting and climate research purposes. The next chapter describes in detail the data used in this study along with the methodology followed. The results are then discussed in the next chapter. A brief summary of the investigation is given in the last chapter.

2. Data and methodology

Sea surface temperatures and wind speeds were downloaded from daily TMI [TRMM (Tropical Rainfall Measuring Mission) Microwave Imager] data available in the website. Specific humidity at air temperature was retrieved from SSMI (Special Sensor Microwave Imager) brightness temperature following Schlussel et al., 1995. Other minor variables like rainfall rate, solar radiation, downwelling Longwave radiation, air temperatures, sea level pressure etc required for the computation of latent heat flux (LHF) were taken from ECMWF daily reanalysis fields. The data taken were then transformed into 5-day, monthly and seasonal averages. Based on the large spatial and temporal variability of air-sea interaction parameters, three broad areas viz: northern Indian Ocean (10^0-20^0N; 60^0-70^0E and 10^0-15^0N; 85^0-90^0E), Equator (5^0-$^-5^0$N and 55^0-95^0E) and South Indian Ocean (10^0- 25^0 S and 55^0-90^0E) were selected over the tropical Indian Ocean. Care had been taken to avoid land contamination while choosing these areas. Computation of LHF was performed using the state of the art COARE 3.0 version of the algorithm published by Fairall et al., 2003 where he claimed that the computational uncertainty is reduced to 5 % level for wind speed < 5 ms^{-1} and to 10 % level for wind speed > 10 ms^{-1}. The COARE bulk flux algorithm has been updated and its range of wind speed validity is extended to 0-20 ms^{-1} . It include improvements to the stability functions, shortening the stability iteration and eliminating the need for a Webb correction to LHF. The modifications were based on nearly 2800 h or direct flux measurements during six cruises augmented with about 100 h of data at wind speeds above 10 ms^{-1} from the HEXMAX experiment.

The latent heat flux as forced by wind speed and air sea humidity difference can be represented by the equation:

$$F_q = L_v \rho C_h U (q_s - q_a) \qquad (1)$$

Where L_v, latent heat of evaporation; C_h, turbulent heat exchange coefficient; ρ, density, U, wind speed at 10m. q_s, sea surface humidity, q_a, humidity at 10m. Differentiating eq. (1) with respect to SST would yield relative importance of dynamic and thermodynamic terms.

$$\frac{\partial F_q}{\partial T_s} = L_v \rho U Dq \frac{\partial C_h}{\partial T_s} + L_v \rho C_h Dq \frac{\partial U}{\partial T_s} + L_v \rho C_h U \frac{\partial Dq}{\partial T_s} \qquad (2)$$

Where Dq = ($q_s - q_a$) is the humidity difference. Here C_h can be considered constant with respect to SST. Hence the variation in LHF is mainly determined by variation of the wind forcing term and humidity difference term.

3. Result and discussion

Using the data from the buoys of the TOGA TAO array in the equatorial Pacific, Zang and Mc Phaden 1995 showed that LHF increases with SST in a linear fashion for SSTs lower than 27^0C and the relationship reverses for higher SSTs. He further summarizes that at low SSTs, variations in surface evaporation are determined primarily by thermodynamics as manifested by the changes in Dq whereas at high SSTs, variations in evaporation are determined by atmospheric dynamics as manifested by changes in WS. The north-south variation of SST, WS and Dq over the tropical Indian Ocean has unique characteristics due to the geography of the region and hence it is worthwhile to investigate the dynamics and thermodynamics along with its seasonal variability. The manifestation of ocean atmosphere coupling with the formation of a LHF maxima in response to the dynamical and thermo-dynamical interaction as shown by Sui et. al 1991 and Zang and Mc Phaden, 1995, was observed in all three regions in the tropical Indian Ocean irrespective of seasons. The scatter plots at these locations exhibited the above trend in spite of the considerable scatter (not shown). In order to highlight the trend the Latent Heat Fluxes were binned into each 1^0C SST interval and the extent of scatter was denoted by the standard deviation (Figs. 1-3). Similarly the WS and Dq were also binned and presented in the diagram (in-set).

3.1. Tropical Indian Ocean

The mean position of the scatter over the North Indian Ocean during northern summer and winter representing the years 2004 and 2007 resembled that of the equatorial Pacific where the SST-LHF trend reversed at 27.5^0C as mentioned in Zang and Mc Phaden 1995. In spite of being a good monsoon year, the LHF maximum was less in 2007 (rainfall 106% of the Long Period Average (LPA)) than those of the weak monsoon year of 2004 (rainfall 87% of LPA) (Figs. 1a&b). However the latent heat fluxes during winter were comparable to each other (Figs. 1c&d). Although the WS during summer in both years was higher than winter, the exceptionally higher LHF in winter probably associated with the relatively higher Dq. It is interesting to note that the high LHF in winter is the result of the optimum SST-WS-Dq (~28^0C - ~5 ms^{-1} - ~7-8 g/kg) combination as reported by Muraleedharan et al. 2006.

The trends of the mean SST-LHF scatter during summer closely resembled with SST-Dq trend in both years while the wind showed an inverse linear trend. On the contrary the SST-LHF trend in winter resembled more to the SST-WS scatter and was true for both years. In short, the variations in surface LHF were determined by thermodynamics as manifested by the changes in Dq during summer whereas the variations were determined by dynamics during winter as manifested by the changes in WS (Fig.1). This was in contrast to the observations of Zang and Mc Phaden 1995 that thermodynamics controlled the process over the equatorial Pacific when SST was less than 300K beyond which the dynamics decided the fate of evaporation. But a closer look at the relative contribution of wind speed and humidity gradient on the total LHF variability derived from equation (2) and illustrated in Table 1 revealed the collective importance of both WS and Dq in understanding the nature of forcing. It was observed that dynamical control over equatorial Pacific was only less than 30 % of the thermodynamics when SST was less than 300 K whereas it was more than half of thermo dynamical control when SST was greater than 300 K. Contrary to these observations, thermo dynamical contribution over the north Indian Ocean was about 3 times the dynamics during summer when SST was less than 27.5^0C but both acted in the opposite direction. This was true for both years. But when SST was above 27.5^0C, dynamical control dominated over thermodynamics unless the thermodynamic supported dynamics as seen in the summer of 2004 (Fig. 1). Interestingly, during winter season, dynamical control dominated on either side of the threshold SST irrespective of the year.

The overall pattern of scatter at the Equatorial Indian Ocean resembled that of north where the LHF seemed to be peaking at the threshold SST of 27.5^{0}C with definite inter annual signals. The mean trend of the scatter indicated less seasonal variability of WS and Dq compared to the northern basins. A strong inter annual signal arising from the 2007 dipole was instrumental in the disappearance of usual SST-LHF structure during 2007 summer (Fig. 2b). In winter the trend did persist in 2007 at least in the warmer half but the absence of similar trend in 2004 represented the decoupled ocean-atmosphere system as explained by Sui et. al (1991). The variation of LHF with SST was controlled more by thermodynamics (almost 50% more) at low SSTs (< 27.5^{0}C) during summer months of 2004 (Table.1). During 2007 summer SSTs had never gone below 27.5^{0}C as the year witnessed strong dipole event in which the warm water pushed to the west by the prevailing walker circulation. This warm water intrusion subdued the effect of ambient cold water at the western equatorial region. As the SST become warmer than 27.5^{0}C, variation of LHF with SST was determined more by atmospheric dynamics as manifested by the slope of WS term irrespective of season.

Mean LHF binned at 1^{0}C SST interval has demonstrated the same pattern of variability over the South Indian Ocean with LHF increased linearly with SST in the lower SST regime and then decreased with further increase in SST. The reversal of LHF-SST relationship, the sign of ocean-atmosphere coupling, occurred at much lower temperature (~23.5^{0}C) at these latitudes during summer (Fig. 3a). The magnitude of LHF-maximum was higher in 2004 than in 2007 which appeared to be in accordance with the higher WS-peak observed in 2004. However the trend of Dq did not show any significant inter annual variability. In spite of the striking inter annual signals, the LHF peak consistently observed at 23.5^{0}C (Fig. 3a) indicating that the ocean atmosphere coupling was highest at this temperature in these latitudes. A closer look at these graphs revealed that the evaporation at this region was primarily determined by dynamics as manifested by the change in WS at low SST regime whereas the variation in surface evaporation at high SST regime was determined by thermodynamics as manifested by the change in Dq. This was in contradiction with the concept explained at north/equator and also by Zang and Mc Phaden 1995 at the equatorial Pacific where the influence of dynamics and thermodynamics were felt at higher and lower SST regimes respectively. It is worthwhile to analyze the relative importance of WS and Dq in controlling the surface LHF during summer. At low SST (< 23.5^{0}C), $\partial U / \partial T_s$ overcame the inverse effect of $\partial Dq / \partial T_s$ in generating LHF to effect a linear increment during 2004 whereas in 2007 both $\partial U / \partial T_s$ and $\partial Dq / \partial T_s$ collectively supported the linear trend although the contribution of $\partial Dq / \partial T_s$ was relatively weak (Table.1). However at high SST (> 23.5^{0}C) $\partial Dq / \partial T_s$ contribution was remarkable in both years during summer and the contribution from $\partial U / \partial T_s$ was almost negligible (< 15%). In short evaporation at these latitudes is primarily determined by both dynamics and thermodynamics and for optimum production of evaporation an ideal combination of WS and Dq was established at the threshold SST of 23.5^{0}C. The subsidence at the subtropics bring cold dry wind to north to meet strong easterly trade wind thereby compromising with ideal wind speed-Dq combination to generate high LHF at an available SST of 23.5^{0}C. It is interesting to note that the dynamic/thermodynamic criteria swapped lower and higher SST regime while shifting from northern to southern sectors of Indian Ocean. The inter-annual variability of the magnitude of LHF during winter months largely depended on the magnitude of Dq as the WS does not exhibit any drastic change. This dependency was also visible in the northern Bay during summer and winter months where the magnitude of LHF fluctuated with the magnitude of humidity gradient (Fig.1). The abnormal reduction of LHF variation in the low SST regime (< 27^0C) was supported by equally low Dq variability but the LHF variation in the warm SST regime (> 27^0C) was influenced by WS variability. The results in table 3 indicated that at high SST, LHF variations were determined primarily by dynamics whereas in the low SST regime, the variations were determined more by thermodynamics. The results, therefore, defies the dynamic and thermodynamic considerations suggested by Ramnathan and Collins (1992) and also Neelin and Held (1987) and Liu (1988), that at high SSTs surface air is convectively unstable, there by subjecting it to low level convergence and at the centre of convergence the wind speed is low limiting LHF.

3.2. Sea level pressure and SST-LHF variability

The zonally averaged annual MSL pressure varied about 1 mb between 2004 and 2007 over the tropical Indian Ocean and the gap widened in the sub tropics (Fig.4). But the rate of change of LHF with pressure in both space and time was negligible. Zonal average of SLP and SST during both summer and winter months of 2004 and 2007 from 25^0N to 30^0S indicated an association between SLP and SST as the variation of pressure had an inverse reaction to SST during both summer and winter at time exhibiting substantial inter annual variability. This is further demonstrated by displaying the linear regression coefficient between SST and SLP over the three domains during these two years (Table 2). A strong inverse correlation was noticed between SST and SLP over the southern Indian Ocean without much inter-annual signal. The correlation appeared to be more consistent during the winter season over the entire tropical Indian Ocean. However the relationship degrades over equatorial and north Indian Ocean during boreal summer irrespective of the year. In Fig. 5 the LHF contours were plotted against SST and SLP over the tropical Indian Ocean during summer for the years 2004 and 2007. The diagonally orientated high LHF contours exhibited an inverse trend between SST and SLP, indicating the shifting of LHF maxima towards lower SST regime as SLP increases and the shifting was more pronounced in the southern latitudes (south of 10^0S). But at the equator and north the threshold-SST at which the LHF start decreasing with SST as a mark of coupled air-sea boundary remained to be between 27^0 and 28^0C. Similar thresholds were observed at the equatorial Pacific by Zang and Mc Phaden 1995 because both equatorial Pacific and northern Indian basins come under the same pressure band especially during the monsoon months. This agrees well with the results of Laird and Kristovich 2002 who suggested the magnitude of surface heat and moisture fluxes remained coupled to transient synoptic-scale weather events (as identified by sea level pressure). The increase (decrease) of LHF with SST in the lower (higher) SST regime was attributed to enhanced air-sea coupling explained by Sui et al. 1991 and Zang and Mc Phaden 1995. The shifting of LHF maxima is even visible in the northern basin (< 1006 mb; ~28^0C) especially over Arabian Sea. Bay of Bengal, being warmer than Arabian Sea by about 1^0C, produced less LHF to leave a vertical patch between 1000 and 1009 mb pressure contours. The rate of increase of LHF with pressure in the northern ocean was much less than the south with minimum SST variability as the LHF contours (< 1012 mb) ran more or less parallel to the pressure axis. The winter months, however, did not show any interesting pattern as the SLP and SST at the higher latitudes depicts the same patterns and exhibited a mixed response of both north and south (figure not shown).

4. Summary

The dynamic and thermodynamic behavior of the northern and equatorial Indian Ocean (north of 10^0S) was explained from the interplay of wind speed and humidity gradient on either side of a threshold SST of 27^0–28^0C by virtue of air-sea coupling suggested by Ramanathan and Collins (1992) and Sui et al. (1991). However, in winter, the slope of the curve on either side of the threshold SST indicated the dominance of dynamical term north of 5 S. The close resemblance in dynamic/thermodynamic behavior of equatorial Pacific and the northern Indian basin was due to the fact that both regions fall under the same pressure band as seen from MSL pressure maps (not shown). Nevertheless, the dominance of thermodynamic forcing (dynamic forcing) was evident in the colder side (warmer side) of the threshold in boreal summer in the northern hemisphere and the situation reverses in the southern hemisphere. The manifestation of enhanced air-sea coupling was noticed in the southern latitudes in the form of high LHF at various combinations of SLP and SST (as both varied drastically with space) so that LHF peak shifted to the higher SST regime as the SLP decreased. The shift is consistent and predominant in both 2004 and 2007. The strong correlation observed between SST and SLP especially over the southern Indian Ocean support the role of SLP in modifying the thermodynamic forcing that appears to be dominating the air-sea interaction processes. These results consolidate the role of transient synoptic-scale weather events like SLP in modulating dynamic and thermodynamic forcing in a coupled ocean-atmosphere system. Why such shifting was not observed north of 10^0S is a point to ponder? At a closer look, the shifting of LHF maxima was even visible in the northern basin (< 1006 mb; ~28^0C) especially over Arabian Sea. Bay of Bengal, being warmer than Arabian Sea by about 1^0C, produced less LHF to leave a vertical patch between 1000 and 1009 mb pressure contours. The rate of increase of LHF with pressure in the northern ocean was much less than the southern ocean with minimum SST variability as the LHF contours (< 1012 mb) ran more or less parallel to the pressure axis. It was also observed that the thermodynamics played decisive role at the north in the lower SST regime in generating LHF through air-sea coupling while at south the role of dynamics was dominant in the lower SST regime to produce similar air-sea coupling. However the situation reversed in the warmer SST regime. At the equator (10^0N – 10^0S), milder air-sea coupling generated less LHF compared to the north and south and the reason for such reduction was attributed to the less humidity gradient at the equatorial Indian Ocean. The shifting of LHF peak was sharper when the air-sea coupling was stronger as seen in southern latitudes. Shifting was absent at the equator when the coupling was relatively weaker.

Acknowledgement

We thank the Director, National Institute of Oceanography, Goa and the Director, Indian National Center for Ocean Information Services, Hyderabad for facilities and funds to undertake the work. We also thank Dr. Frank Wentz and his office ‘Remote Sensing Systems’ for providing SSMI and TMI products. ECMWF ERA-Interim data used in this study/project have been provided by ECMWF/have been obtained from the ECMWF data server. This is NIO contribution number *****.

References

FAIRALL, C. W., BRADLEY, E.F., HARE, J.E., GRACHEV, A.A. and EDSON, J.B.., 2003, Bulk Parameterization of Air-Sea Fluxes: Updates and Verification for the COARE Algorithm. *J. of Climate*, **16**, pp. 571-591.

LAIRD, N.F., and DAVID A. R. KRISTOVICH., 2002, Variations of sensible and Latent Heat Fluxes from a Great Lakes Buoy and Associated Synoptic Weather Patterns. *J. Hydrometeorology*., **3**, pp. 3-12

LIU, W. T., 1988, Moisture and latent heat flux variabilities in the tropical Pacific derived from satellite data. *J. Geophys. Res*., **93**, pp. 6749-6760.

MURALEEDHARAN, P.M., PANKAJAKSHAN, T., SATHE, P.V., MURTY, V.S.N. and SANTHOSH, R., 2006, Monsoonal reversal of Remote Sensing Biases of Latent Heat Flux over the Eastern Arabian Sea. *Geophys. Res. Let*, **33**, LI8605, doi:10.1029/2006GL026093, 2006.

MURALEEDHARAN, P.M., and PANKAJAKSHAN, T., 2008, How consistent is the satellite derived SST-LHF relationship in comparison with observed values? *Int. J. Remote Sensing*, **29** (14), pp. 4207 – 4217 (DOI: 10.1080/01431160701840190).

NEELIN, J. D., and HELD, I. M., 1987, Modeling tropical convergence based on the moist static energy budget. *Mon. Wea. Rev*., **115**, pp. 3-12.

RAMANATHAN, V., and COLLINS, W., 1992, Thermostat and global warming. *Nature*, **357**, 649.

SCHLUSSEL, P., SCHANZ, L., ENGLISCH, G.., 1995, Retrieval of Latent Heat Flux and Longwave irradiation at the sea surface from SSM/I and AVHRR measurements. *Adv. Space Res*., **16**, pp. (10)107-(10)116.

SUI, C.-H., K.-M. LAU, and BETTS, A. K., 1991, An equilibrium model for the coupled ocean-atmosphere boundary layer in the tropics. *J. Geophys. Res*., **96**, pp. 3151-3163.

ZANG, G J and MCPHADEN., 1995, The relationship between Sea Surface Temperature and Latent Heat Flux in the Equatorial Pacific. *J. of Climate*, **8**, pp. 589-605.

Table

Table 1. Linear regression slopes w.r.t. SST in the Tropical Indian Ocean during summer and winter of 2004 and 2007.

Year	Season	Area	Threshold (°C)	[illegible]	∂Pa	∂U	Threshold	[illegible]	∂Pa	∂U
2004	Summer	NIO	< 27.5	12.83	15.94	-5.21	> 27.5	-17.74	-7.28	-8.19
		EIO	< 27.5	4.67	8.95	-5.90	> 27.5	-6.83	4.96	-13.37
		SIO	< 23.5	5.22	-4.84	11.59	> 23.5	-39.09	-27.21	-3.76
	Winter	NIO	< 27.5	5.47	-3.82	8.63	> 27.5	-6.33	-0.90	-5.66
		EIO	< 27.5	-	-	-	> 27.5	2.24	3.82	-2.85
		SIO	< 27.5	1.74	1.87	-0.12	> 27.5	-6.24	3.83	-11.59
2007	Summer	NIO	< 27.5	13.01	18.16	-6.39	> 27.5	-4.01	3.27	-7.97
		EIO	< 27.5	-	-	-	> 27.5	-7.39	6.71	-13.97
		SIO	< 23.5	17.49	5.09	10.71	> 23.5	-20.75	-20.49	-2.80
	Winter	NIO	< 27.5	13.98	-2.88	21.55	> 27.5	-13.01	1.89	-14.56
		EIO	< 27.5	-	-	-	> 27.5	-14.69	-1.63	-12.96
		SIO	< 27.5	2.79	-1.17	6.93	> 27.5	-21.08	-6.66	-11.76

FIGURE 1

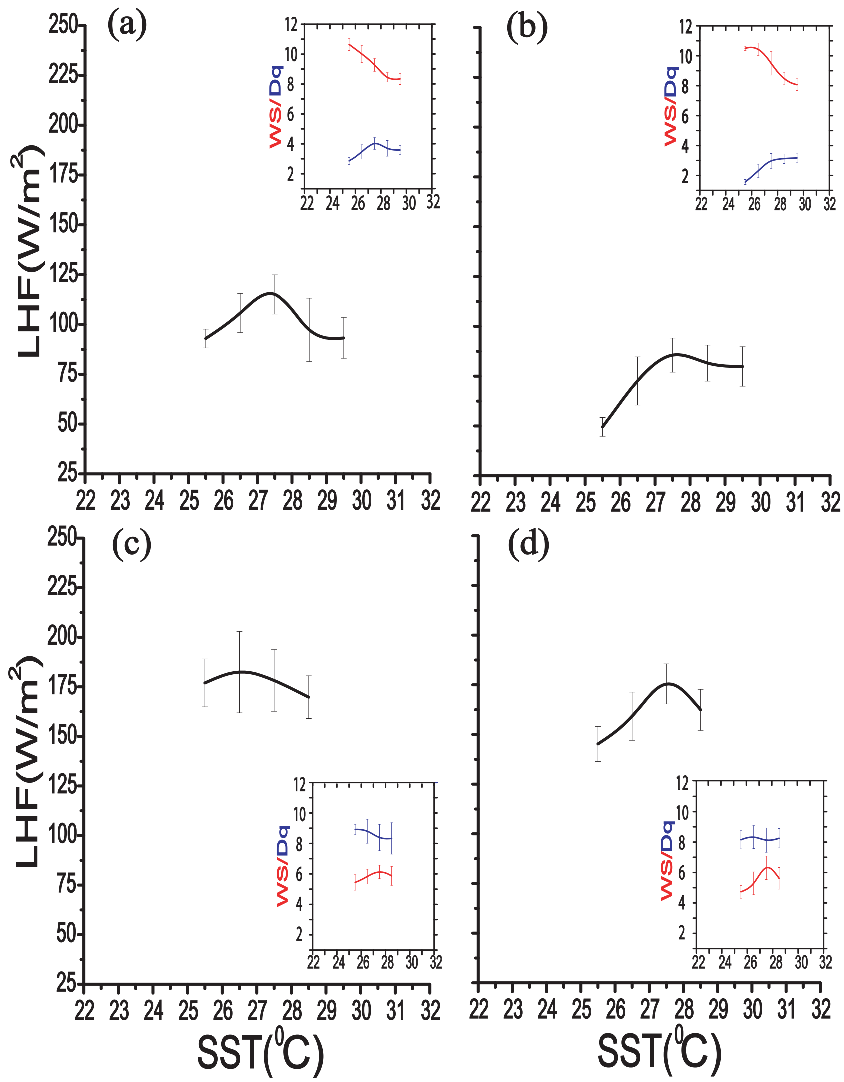

Figure 1. Binned scatter plots between LHF and SST in the North Indian Ocean during summer (a&b) and winter(c&d) of 2004 (left panel) and 2007 (right panel). Plots of WS and Dq are given in the inset. Vertical line indicates standard deviation.

FIGURE 2

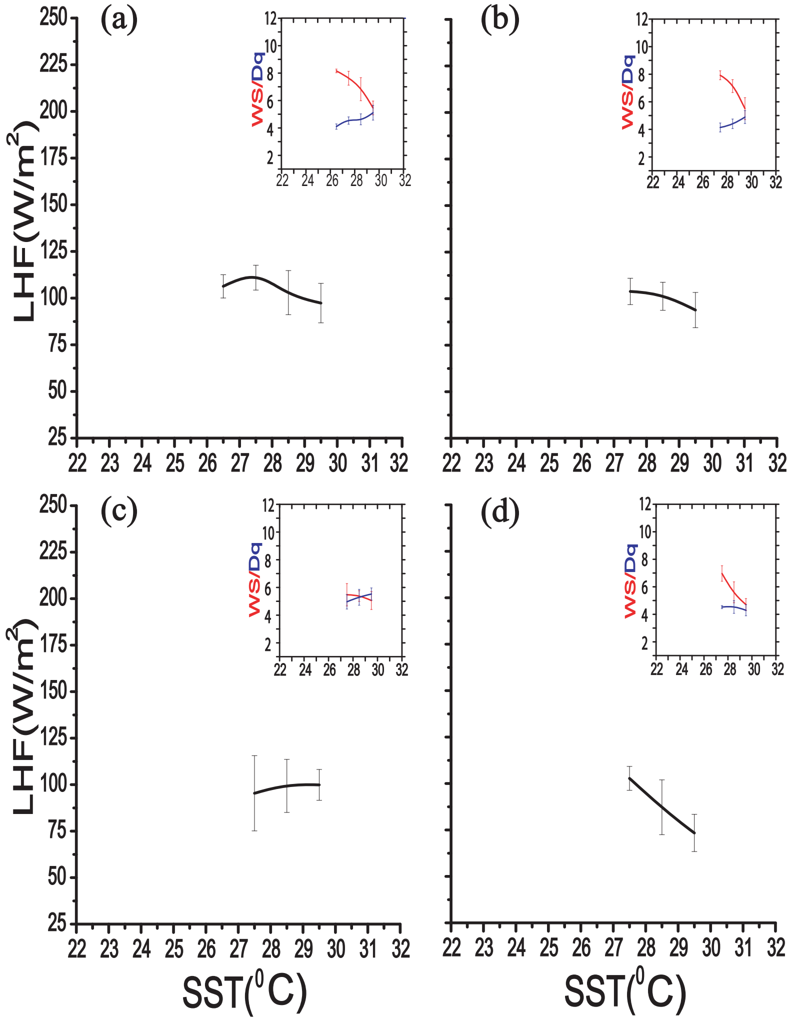

Figure 2. Binned scatter plots between LHF and SST in the Equatorial Indian Ocean during summer (a&b) and winter(c&d) of 2004 (left panel) and 2007 (right panel). Plots of WS and Dq are given in the inset. Vertical line indicates standard deviation.

FIGURE 3

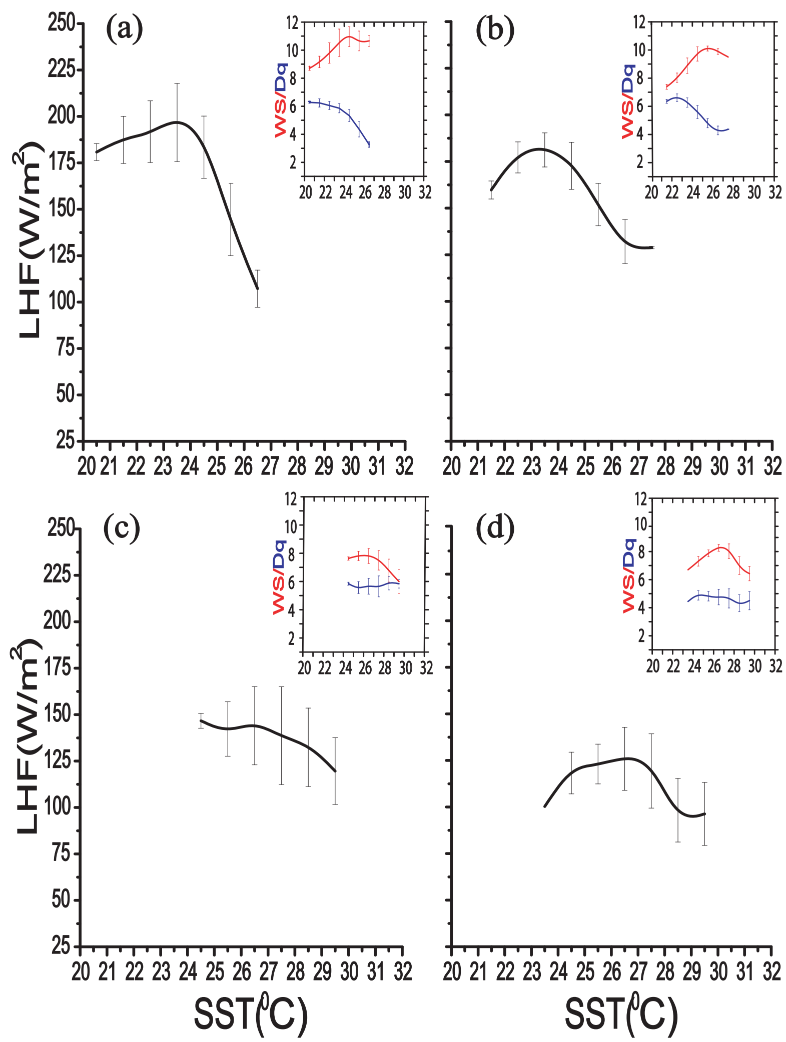

Figure 3. Binned scatter plots between LHF and SST in the South Indian Ocean during summer (a&b) and winter(c&d) of 2004 (left panel) and 2007 (right panel). Plots of WS and Dq are given in the inset. Vertical line indicates standard deviation.

FIGURE 4

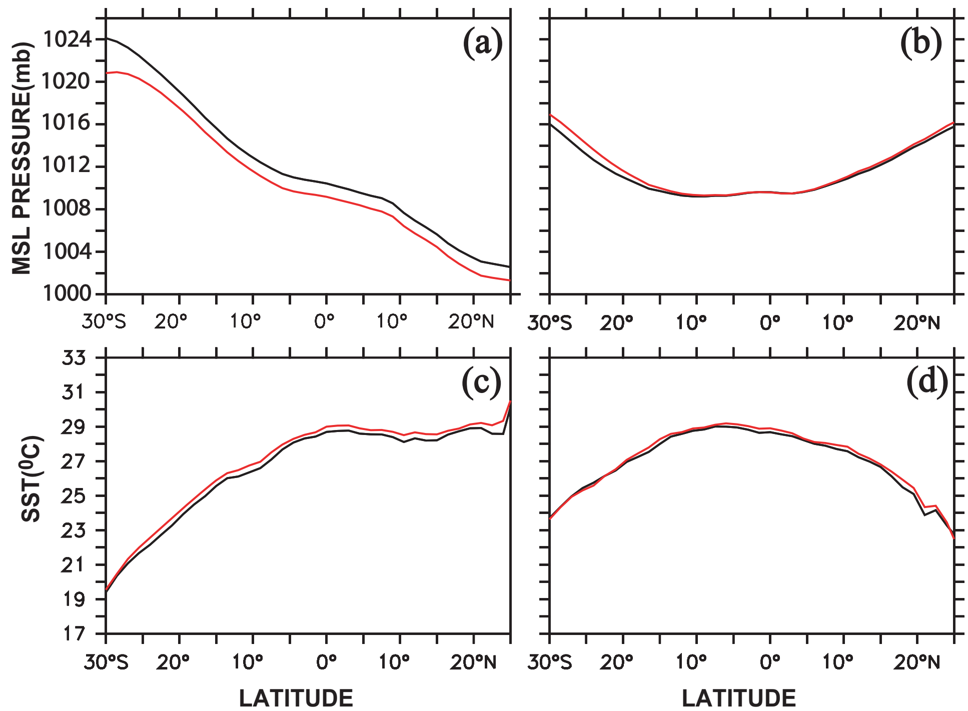

Figure 4. Latitudinal variation of MSL pressure and SST over Indian Ocean during Summer (a&c) and Winter (b&d) of 2004 (black) and 2007 (red).

	Linear Regression coefficient (SST Vs SLP)					
	Northern Hemisphere Summer			Northern Hemisphere Winter		
	NIO	EIO	SIO	NIO	EIO	SIO
2007	-0.37 (178)	-0.32 (400)	-0.93 (525)	-0.83 (178)	-0.52 (400)	-0.94 (525)
2004	-0.40 (178)	-0.42 (400)	-0.93 (525)	-0.93 (178)	-0.88 (400)	-0.94 (525)

Table 2. Linear Regression Coefficient between SST and SLP over North Indian Ocean (NIO), Equatorial Indian Ocean (EIO) and South Indian Ocean during 2004 and 2007.

FIGURE 5

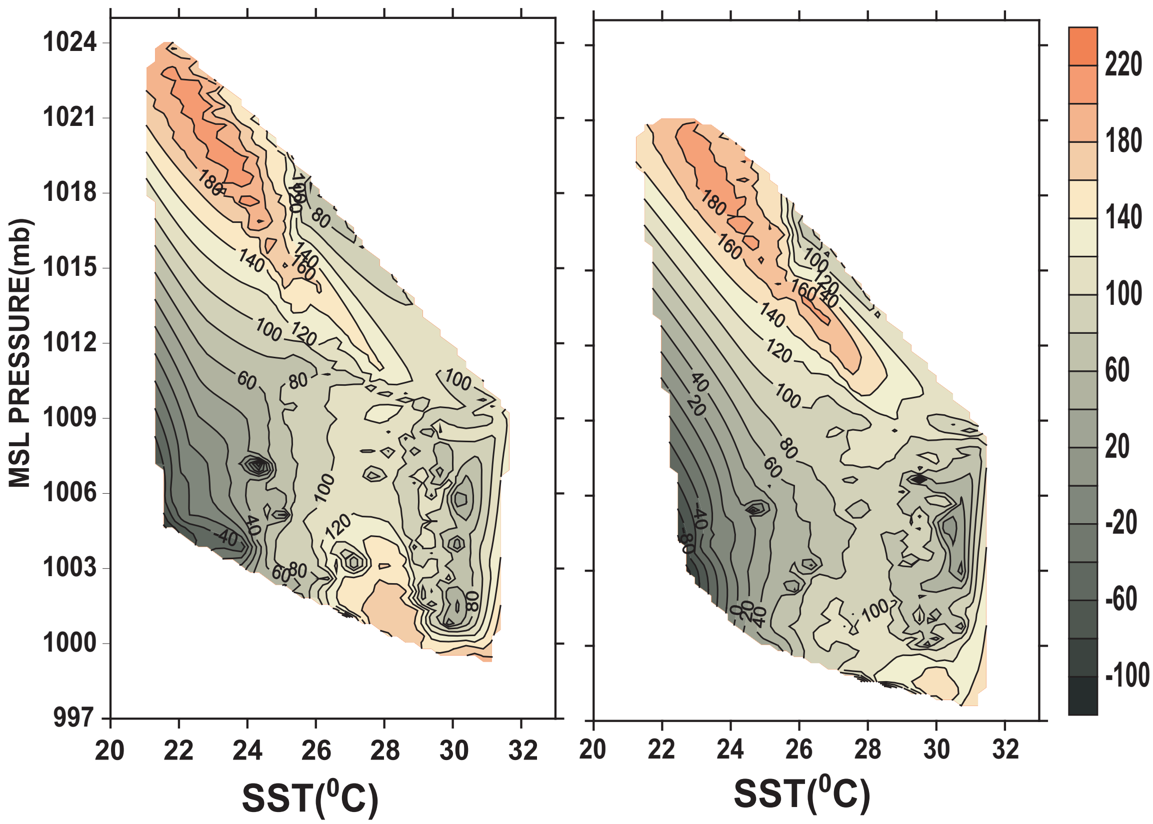

Figure 5. Variation of LHF as a function of MSL pressure and SST over Indian Ocean during summer of 2004 (left panel) and 2007 (right panel).